ACS OMEGA

http://pubs.acs.org/journal/acsodf

Article

Complete System to Generate Clean Water from a Contaminated Water Body by a Handmade Flower-like Light Absorber

Muhammad Javed, Sippi Pirah, Yonghe Xiao, Yilan Sun, Yating Ji, Muhammad Zubair Nawaz, Zaisheng Cai, and Bi Xu*

Cite This: *ACS Omega* 2021, 6, 35104–35111

Read Online

ACCESS | Metrics & More | Article Recommendations | Supporting Information

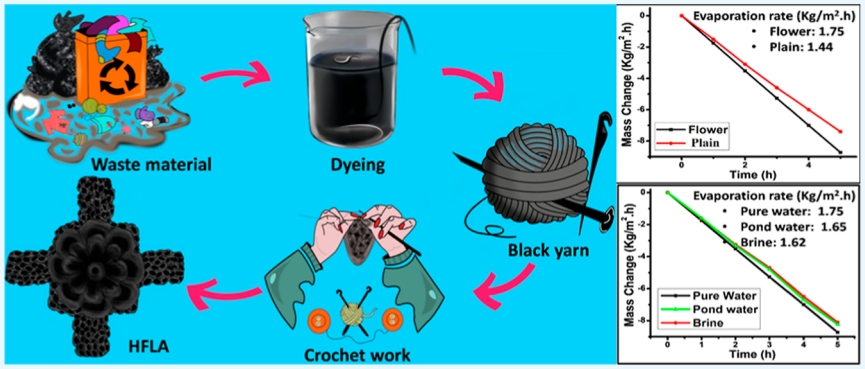

ABSTRACT: The utilization of solar energy to make human lives better has been one of the primary and green approaches adopted by ordinary people and researchers for decades. This approach has recently gained a lot of attention as a way to tackle clean water scarcity in remote areas. Costly components, complex manufacturing procedures with rarely available equipment, and a surface to condense water vapors are challenges in the way of its application in the required areas. Here, we propose a complete system to solve this problem with a handmade light absorber and a superhydrophilic surface (antifogging) to get vapors back to collect clean water. Our handmade flower-like light absorber stitched by crochet work, the single stitch method, was able to get a decent evaporation rate of 1.75 kg/m^2·h in pure water and slightly lower rates of 1.62 and 1.65 kg/m^2·h with brine and pond water, respectively. Still, our proposed superhydrophilic coated surface can collect ∼37% more water than the pristine surface. This system has a huge potential for use in rural areas because of multiple key advantages, such as simple technology, readily available low-cost raw materials, and easy fabrication.

1. INTRODUCTION

Sunlight (solar energy) is a vital part of our ecosystem. It plays an integral role in many biological activities. Learning from Mother Nature, humans also have a long history of taking advantage of this abundantly available energy source to make their lifestyle better and healthier.[1−4] Due to massive industrialization and climate change in the past few decades, clean water scarcity has become an alarming challenge for humanity's healthy survival, especially in rural areas.[5] Addressing this challenge in remote areas with solar energy has become one of the feasible and green approaches adopted by researchers from the past few years.[6−11]

Traditional heating methods lose their efficiency because of heat dissipation in bulk water, leading to neglectable or meager evaporation rates.[12] In contrary to conventional heating behaviors, the interfacial localized heating technique has gotten a huge appreciation recently.[13−15] This technique has the perk of localizing solar heat energy at the air−water interface, ultimately resulting in much better evaporation rates.[16,17] Recently, extensive efforts have been made to fabricate efficient, low-cost, and reliable solar light absorbers, such as solar-trackable super-wicking black metal panels, plasma-made graphene nanostructures, carbon nanotube composite polyacrylamide hydrogel, and so forth.[18−20] Especially, the fabrication of 3D geometric shapes with a rough exterior to increase exposed surface area, which ultimately leads to better solar light absorption and evaporation rates, such as 3D dyed black cotton towel, 3D hemispheric steam generator composed of nano-carbon, 3D spherical carbonized *Platanus* fruit, and so forth.[21−23] However, most of the designed solar light absorbers reported recently are still costly and composed of rare components with complex manufacturing processes.[24] Inter-

Received: October 22, 2021
Accepted: December 1, 2021
Published: December 9, 2021

facial localized heating systems are needed in rural areas, so it is better to be simple and low-cost because the local economy, technical training, and resources of rural areas are limited. It is a worthwhile and practical approach to solve a problem in a specific area by utilizing locally available resources, tools, and technologies. Crochet work is prevalent in different countries, such as Pakistan, China, Bangladesh, India, and so forth and especially in rural areas.[25] People use this art to knit sweaters, scarves, hats, bags, and so forth.

Here, we come up with an easy-to-fabricate handmade flower-like light absorber (HFLA) for solar-driven evaporation. HFLA preparation is excluded from complex equipment, expensive chemicals, and energy resources. We can also utilize outdated and waste clothes (stitched by the crochet method) to get yarn and dye them with black color to acquire raw material. In this way, we can also contribute to the sustainability of the green environment and cut off the raw material capital cost. By using black yarn and a crochet hook, HFLA is stitched by the single stitch method. The fabrication procedure is schematically illustrated in Figure 1. The single stitch method is prevalent,

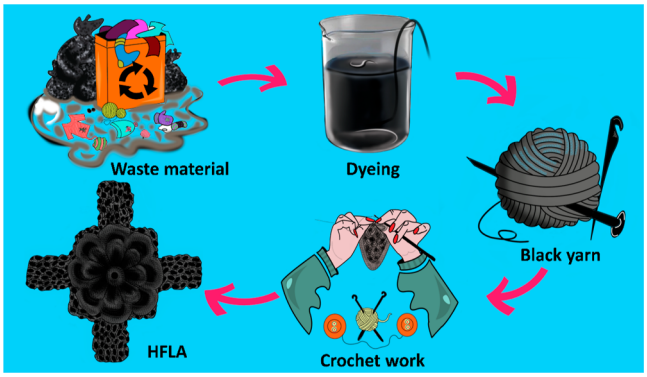

Figure 1. Schematic illustration of the knitting route of HFLA from waste material or black yarn.

accessible, and feasible.[26] Our knitted HFLA is able to get a decent evaporation rate of 1.75 kg/m^2·h in pure water and a slightly lower 1.62 and 1.65 kg/m^2·h with brine and pond water, respectively. Furthermore, the majority of the research in this field has only concentrated on how to improve the evaporation rate, despite generating clean or drinking water, which is not that much in earnest. Coating plays an important role to improve the properties of a material.[27,28] Here, we proposed a super hydrophilic coating to collect water vapors back efficiently while keeping the coated surface transparent. In this way, sunlight can easily reach out to the light absorber to keep evaporation continuing smoothly. The prepared coated surface dome over HFLA is able to collect 0.51 kg/m^2·d water, which is ∼37% more than the pristine surface water collection.

Our proposed handmade solar evaporator and complete system with superhydrophilic coated surface have various applications from the industrial to the household level such as wastewater treatment, low-temperature steam production, and generation of clean water from a contaminated water body. It can also support the economy of rural areas by selling HFLA to small industries for wastewater treatment.

2. EXPERIMENTAL SECTION

2.1. Materials. Black yarn (80% long-staple cotton, 20% milk fiber) was provided by Sheng Tang Textile Co. Ltd. (Shanghai-Qidong, China); crochet hook (I-9, metric diameter 5.5 mm) was purchased from JIDI Tools Co. Ltd (Zhejiang-Jinhua, China); pectin [galacturonic acid (dry basis) ≥74.0%] was provided by Sinopharm Chemical Reagent Co. Ltd. (Ningbo, China); tannic acid was purchased from Shanghai Yishi Chemical Co. Ltd (Shanghai, China); and cola bottle (PET, polyethylene terephthalate) was purchased from Family Mart (Shanghai, China). Sodium chloride (NaCl) was purchased from Shanghai Ling Feng Chemicals and Reagent Co. Ltd.

2.2. Preparation of Super Hydrophilic Coating (Anti-fogging). A super hydrophilic (antifogging) coating was prepared by mixing tannic acid and pectin aqueous solutions in a fixed volume ratio according to the previously published work.[29] First, we prepared a tannic acid (3 wt %) solution in distilled water, and an aqueous solution of pectin (3 wt %) was also prepared using the same method. After getting well-homogenized solutions, they were mixed in a 1:1 ratio until they turn into a sticky and viscous liquid. The final liquid was poured in a half-cut cola bottle (PET) at the inner side until it covered its internal surface evenly. Finally, the cover (dome) was dried in a dryer at 40 °C for 30 min. After drying, it was used for water collection during the experiment.

2.3. Knitting Procedure of HFLA. Here, we use a medium-sized four-ply black-dyed yarn (80% long-staple cotton, 20% milk fiber) (Figure 2a) and a crochet hook (I-9, metric diameter 5.5 mm) for stitching HFLA. The yarn and crochet hook with

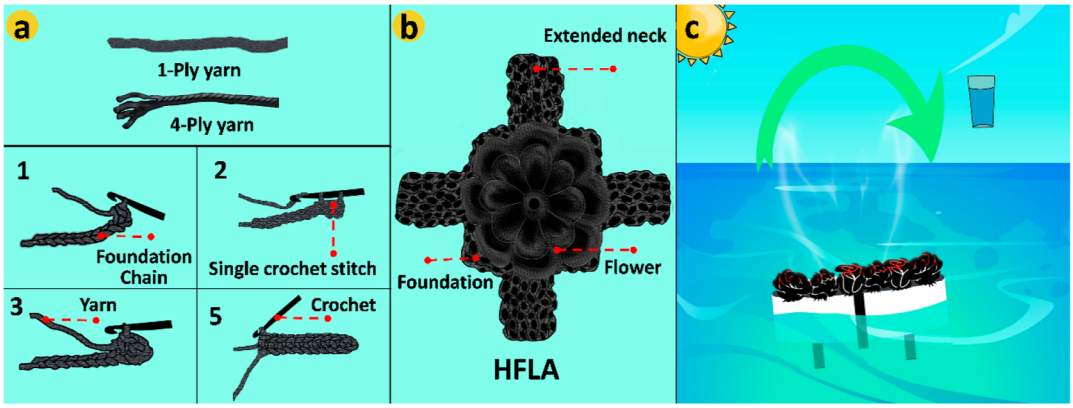

Figure 2. (a) Yarn types and (a2−a5) crochet work single stitch method for knitting HFLA step by step. (b) Parts of HFLA. (c) HFLA outdoor application setup.

https://doi.org/10.1021/acsomega.1c05925
ACS Omega 2021, 6, 35104−35111

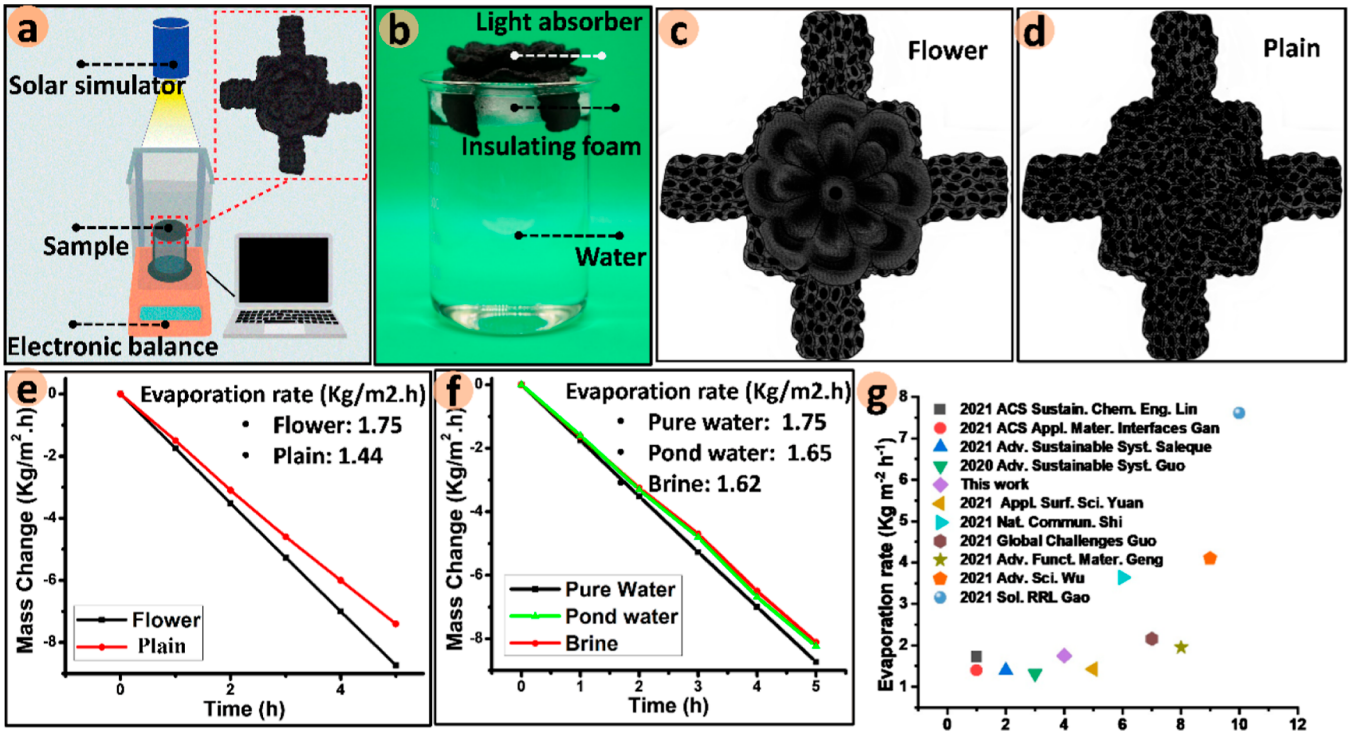

Figure 3. (a) Schematic setup for evaluating the evaporation rate and temperature variations. (b) HFLA, foam, and water arrangements. (c,d) Difference between flower-like and plain evaporator. (e) Evaporation rate of flower-like and plain evaporator. (f) HFLA evaporation performance with pure water, pond water, and brine. (g) HFLA evaporation performance in comparison to other works.

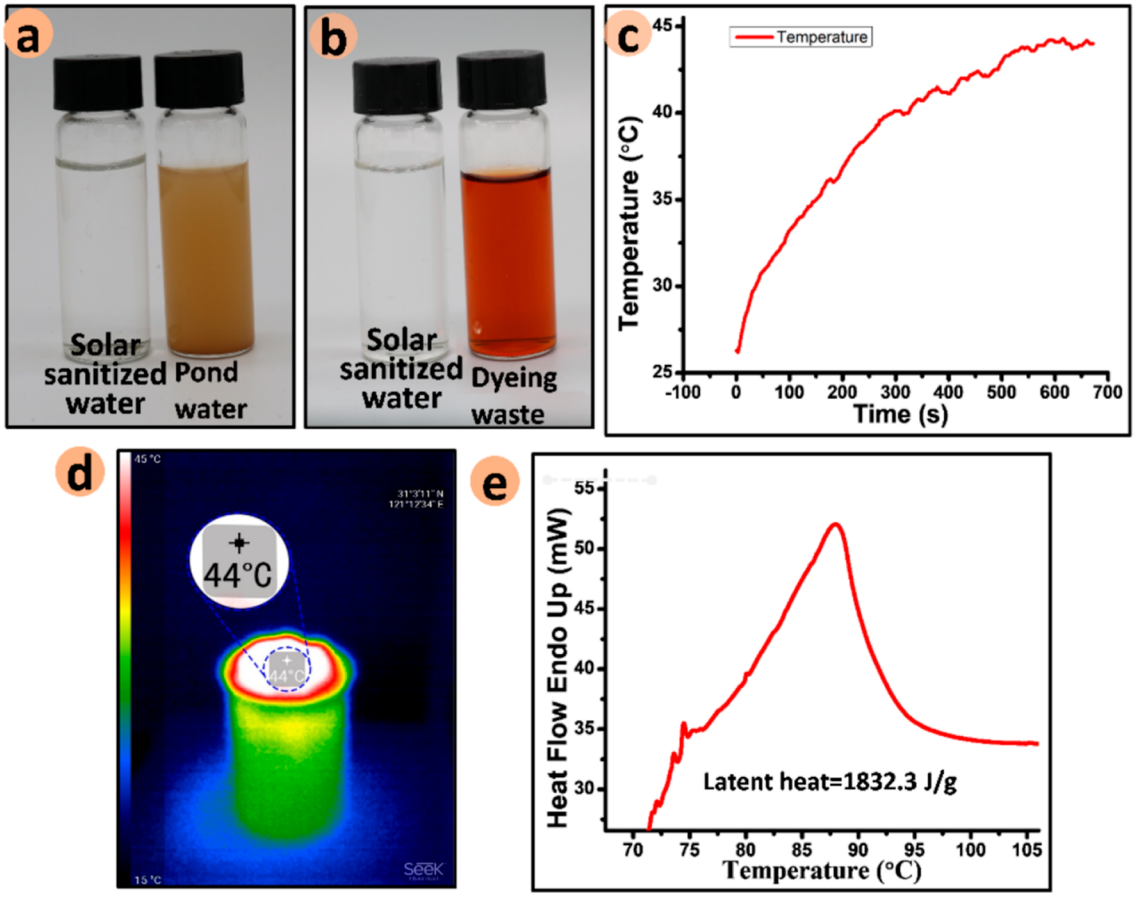

Figure 4. (a,b) Solar sanitized water from pond water and dyeing waste. (c) Temperature variation of the HFLA surface over time under one solar irradiation. (d) Maximum temperature achieved by HFLA surface under one solar irradiation. (e) DCS curve for latent heat measurement.

https://doi.org/10.1021/acsomega.1c05925
ACS Omega 2021, 6, 35104−35111

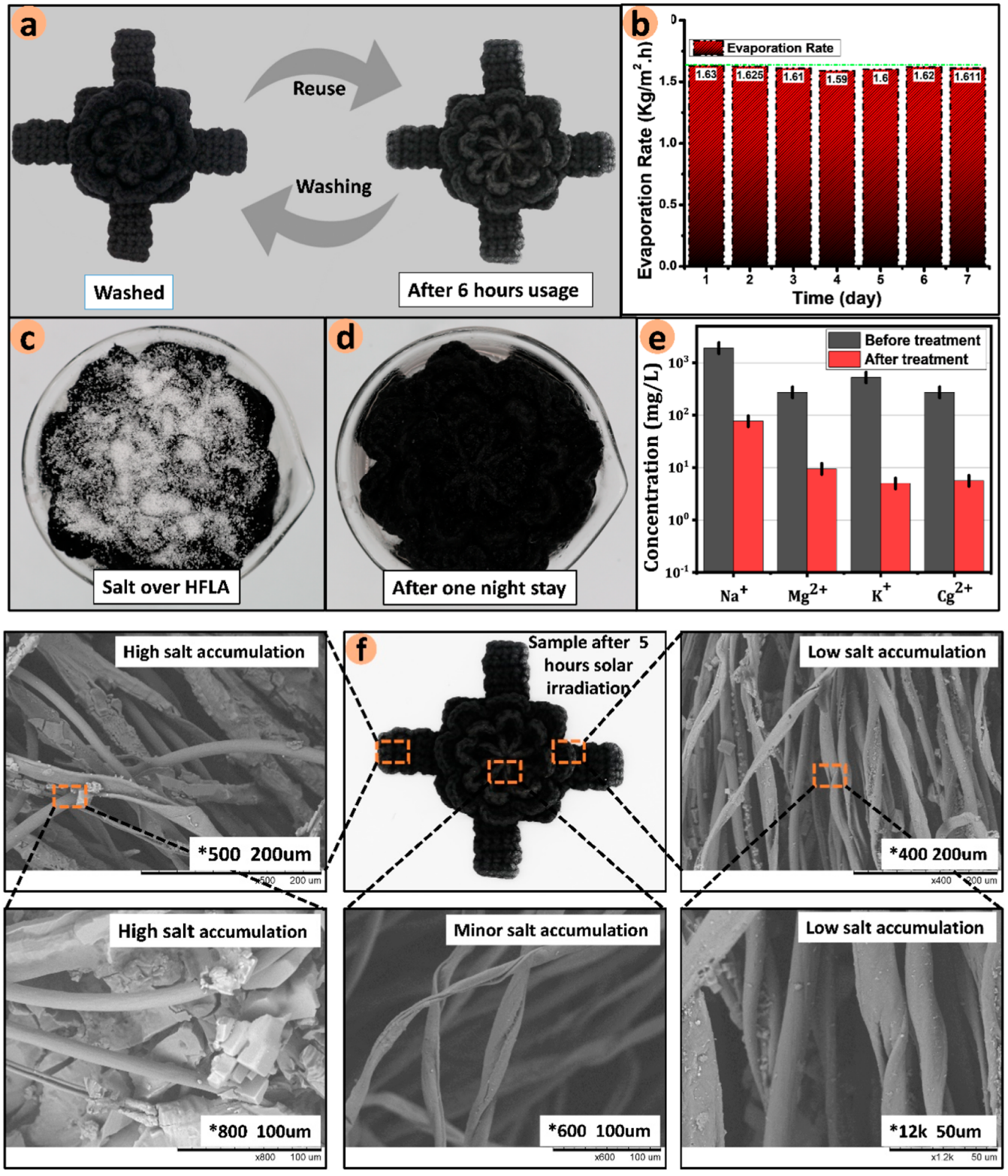

Figure 5. (a) Washing and reuse of HFLA after using over brine. (b) Per day evaporation rate by HFLA over brine under one solar irradiation. (c,d) Demonstration of salt rejection at night. (e) Comparison of ion concentration in water before and after treatment by HFLA. (f) SEM image of different sections of HFLA after using over brine for 6 h.

these specifications are ubiquitous and readily available. We used a single crochet stitch for knitting HFLA, which is a fundamental and straightforward method. The first step is to make a foundation chain and use the single crochet stitch method (demonstrated in steps 1−4) to make the base of the HFLA (see Video S1). The base is square with four extended necks (Figure 2b). These four necks will stay dipped in the body of water and supply ample water for evaporation to the upper surface. The flower is erected in the middle of the square base, which can get an equal water supply from all four extended

https://doi.org/10.1021/acsomega.1c05925
ACS Omega 2021, 6, 35104−35111

necks. The outdoor application setup of HFLA can be seen in Figure 2c.

2.4. Characterization. Differential scanning calorimetry (DSC) was conducted by DSC 8500. The temperature was detected by a thermocouple (DT-8891E, CEM, China) and IR camera (SEEK Compact Pro. Seek Thermal, USA). A solar simulator (PLS-SXE300/300UV, Perfect Light, China) with an intensity of 1 kW m^{-2} was used for solar light irradiation. Different water samples (pure water, pond water, and brine) were used for evaporation rate evaluation. For weight change measurement, an electronic balance (ME204E, Mettler Toledo, USA, accuracy 0.1 mg) was used.

3. RESULTS AND DISCUSSION

The evaporation rate is one of the key factors in determining the effectiveness of an evaporator. We set up an experimental setup to assess the mass reduction or evaporation rate achieved by HFLA. The prepared sample is placed on an electronic balance under a solar simulator, as shown in Figure 3a. The sample consists of HFLA, insulating foam (polystyrene with a thermal conductivity ≈ 0.04 W m/K), and water (Figure 3b). Insulating foam acts as a barrier to the free flow of heat from HFLA to bulk water. As a result, HFLA can achieve a higher temperature, resulting in a better evaporation rate. For the final evaporator, we chose a flower-like structure (Figure 3c) over a plain structure (Figure 3d) (Figure S1, Supporting Information). In terms of evaporation rate, a flower-like evaporator performs better than a plain structure. The plain evaporator has 1.44 kg/m^2·h evaporation rate and the flower-like evaporator has a 1.75 kg/m^2·h evaporation rate (Figure 3e). This is due to the fact that 3D geometric shapes with a rough exterior and a larger exposed surface area absorb solar light efficiently, which ultimately leads to better evaporation rates (Figure S2, Supporting Information).[30] We also tested HFLA's evaporation performance on three different water samples: pure water, pond water, and brine. The evaporation rate for pure water was 1.75 kg/m^2·h, pond water 1.65 kg/m^2·h, and brine 1.62 kg/m^2·h (Figure 3f). The evaporation rate is better with pure water, but even with pond water and brine, the overall evaporation rate remains stable. HFLA's ability to treat a variety of contaminated water is demonstrated by stable evaporation rates with various water bodies. In comparison to other works, HFLA has achieved a satisfactory evaporation rate using simple, accessible, and low-cost technology (Figure 3g). The evaporation rate with pond water and brine is slightly lower because of impurities present in the water body.

The solar sanitized water from pond water and dyeing waste is shown in Figure 4a,b. In order to investigate the temperature variations over time, a thermocouple attached to a computer was used to monitor the temperature variations of the HFLA surface under 1 sun irradiation. When solar irradiation started, the initial temperature of the HFLA surface was 26.4 °C. It reached 44 °C in 583 s or about 10 min (Figure 4c). The maximum temperature achieved by HFLA under steady conditions was also measured by the IF camera, and it was 44 °C (Figure 4d). The pure water latent heat is around 2320 J·g^{-1} under ideal conditions. However, the latent heat of water loaded on HFLA is measured at around 1832.3 J·g^{-1} which is much lower than the pure water in the form of bulk (Figure 4e). Water molecules on the rough surface of HFLA are more likely to escape into the air in the form of tiny water clusters instead of individual molecules from bulk water. Due to this phenomenon, comparatively less energy is required for water molecules to escape the surface.[31]

The photothermal conversion efficiency of HFLA is calculated by the given formula (1).[32]

$$\eta = \dot{m} \times \frac{H_{LV}}{E_i} \tag{1}$$

Here, $\dot{m}$ indicates the evaporation rate due to solar irradiation, which is equal to the evaporation rate measured under solar light (1.75 kg/m^2·h) minus the evaporation rate without a light source (0.132 kg/m^2·h). H_{LV} indicates the total enthalpy, which is the sum of sensible heat (125.9 × 10^3 J·kg^{-1}) and latent heat (1832.3 × 10^3 J·kg^{-1}). E_i is the total input power from xenon light (3.6 × 10^6 J·h^{-1}·m^{-2}). Following the formula, the photothermal conversion efficiency of HFLA under 1 sun irradiation reaches 88%.

Coastal areas also face clean water scarcity because of the high salt content in seawater. We can use seawater for drinking and plantation purposes after expelling the salt and other minerals found in it. According to the factors mentioned above, desalination is also one of the key factors in assessing the solar light absorber performance. Herein, we conducted a series of tests to evaluate HFLA desalination performance. First, the evaporation rate was noted over brine under one solar irradiation to check its evaporation rate stability with time. HFLA was used for 7 days (washing and reuse after 6 h) (Figure 5a). It showed a constant evaporation rate of around 1.61 kg/m^2·h from day 1 to day 7 (Figure 5b). Scanning electron microscopy (SEM) was carried out to check salt deposition on HFLA at its different segments. After 5 h of solar irradiation, there was salt accumulation on HFLA extended necks because they were continuously dipped in brine. The middle section of the HFLA, which is responsible for light absorption and evaporation, acquired minor salt particles (Figure 5f). Salt particles incrementally accumulating on the surface of the HFLA as a result of continuous water evaporation may affect the absorber's optical and wicking attributes, resulting in a lower evaporation rate.[33] Second, solid salt (NaCl) was employed on HFLA under dry conditions (Figure 5c) and placed over pure water for one night (dark conditions, 8 h). There were no salt crystals observed on HFLA the next morning (Figure 4d). Salt crystals moved from the HFLA middle part to bulk water, which was confirmed by measuring the salt content (conductivity) in water before and after the experiment, 650 and 25,000 μS/cm, respectively.[34] Due to the diffusion phenomenon, salt moves from a high-concentrated area (HFLA middle part) to a less-concentrated solution (water). These results show that HFLA has good evaporation performance in brine. Ion concentrations in seawater samples and condensed water were measured to assess HFLA desalination performance. Na^+, Mg^{2+}, K^+, and Ca^{2+} ion concentrations were 1912.2, 273.6, 525.5, and 273.1 mg·L^{-1} in sample, which reduced to 76.9, 9.5, 5, and 5.6 mg·L^{-1}, respectively (Figure 5e). The condensed water quality in terms of ion concentration complied with WHO standards.

The majority of the research in this field has focused on how to get a better evaporation rate.[35] Focusing only on the evaporation rate is not much fruitful. Obtaining clean water for drinking purposes is a critical objective in this research area. To collect sufficient clean water, an efficient surface is required that must be able to condense water $vapors_{(g)}$ into the $water_{(liq)}$ without hindering the sunlight penetration. To get these incentives, the surface must stay transparent. On the contrary, most of the materials get blurred when vapors condense on them and ultimately cause hindrance in the way of sunlight (up to

https://doi.org/10.1021/acsomega.1c05925
ACS Omega 2021, 6, 35104−35111

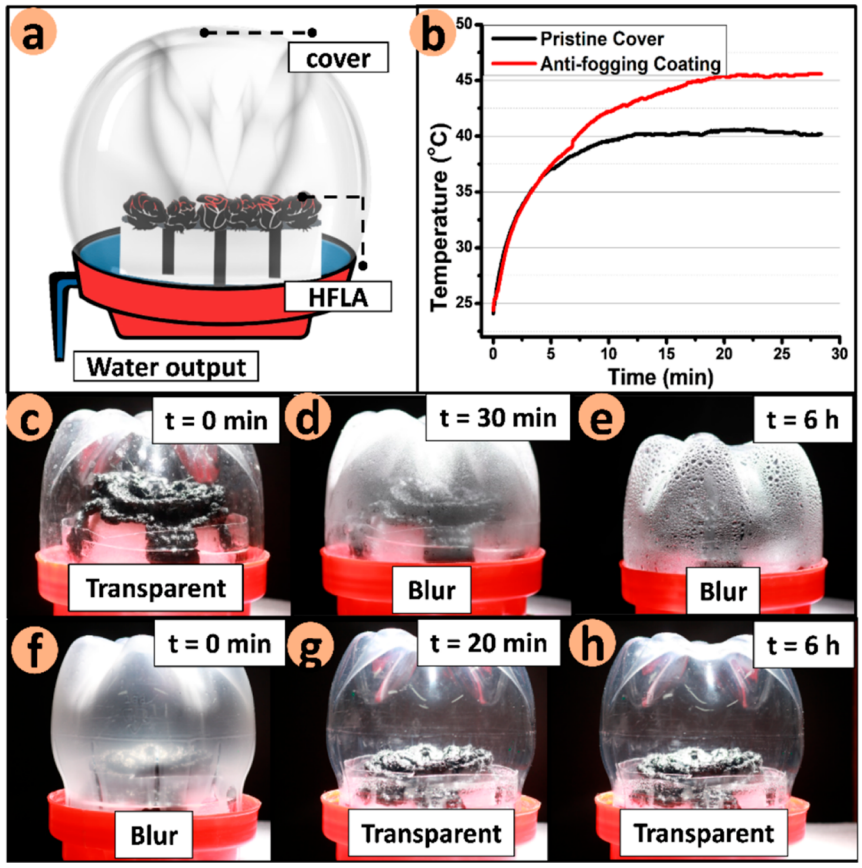

Figure 6. (a) Experimental setup for condensed water collection. (b) Temperature variation of HFLA under one solar irradiation with pristine cover and coated cover. (c–e) Pristine cover surface variation in terms of transparency by water vapor deposition. (f–h) Coated cover surface variation in terms of transparency by water vapors deposition.

35%) reaching out light absorber.[36] Herein, we used superhydrophilic coating on the inner side of the waste cola bottle (PET) to get antifogging properties. The prepared superhydrophilic coating demonstrates film-like condensation while keeping itself transparent. This is because the prepared coating possesses plenty of hydrophilic hydroxyl (−OH) groups. These groups (−OH) on coated PET films stimulate the diffusion of water vapors, leading to reduced water contact angle values. A test setup is arranged to analyze the water collection difference between the coated and uncoated surfaces. HFLA is placed over pond water which is in a bucket. There is an insulating foam in between the HFLA and the pond water while the HFLA extended necks are dipped in water. A dome-like cover is placed on it for water collection by condensation. There is an outlet nozzle at the bottom for clean water collection (Figure 6a). The first test is carried out with a pristine surface under one solar irradiation. At t = 0 min, the surface is transparent, as shown in (Figure 6c). As evaporation starts, the surface becomes blurry due to tiny water droplets (fog) deposition on the pristine surface within 30 min (Figure 6d). Even after 6 h, the surface stays blurry (Figure 6e). For better evaporation, sunlight should reach out to HFLA without any blockage. However, in the case of a pristine surface, a part of the sunlight gets blocked by the foggy layer. On the other hand, the coated surface is blurry at start t = 0 min (Figure 6f). After 30 min, it becomes almost transparent and starts a film-like water collection (Figure 6g). This transparent surface lets sunlight pass through it without any considerable hindrance. In this way, an ample amount of sunlight is able to reach out to HFLA for better and smoother evaporation. The coated surface stays transparent for 6 h (Figure 6h). The HFLA surface temperature difference between a pristine surface and a coated surface is more than 5 °C (Figure 6b). As the pristine surface was transparent at the start, the HFLA surface temperature increased a little faster than the coated surface and ultimately achieved 40 °C. The coated surface becomes transparent with time. That is why the HFLA surface reached 45 °C with it, which is 5 °C more than the pristine surface. The evaporation rate is directly proportional to the surface temperature. The pristine surface water collection rate is 0.32 kg/m^2·d and the coated surface water collection is 0.51 kg/m^2·d, which is ∼37% better than the pristine surface.

4. CONCLUSIONS

In this study, we developed a HFLA by using a crochet hook and black yarn. It is a straightforward and easy strategy for making a light absorber, characterized by reproducibility, high efficiency, and reduced production costs. The raw material is also available without any difficulty in the area where this technology needs to be deployed. HFLA stitched by crochet work, single stitch method, can get a decent evaporation rate of 1.75 kg/m^2·h in pure water and a slightly lower 1.62 and 1.65 kg/m^2·h with brine and pond water, respectively. Furthermore, our proposed superhydrophilic coated surface can collect 0.51 kg/m^2·d water, which is ∼37% more than the water collection of the pristine surface. Due to multiple advantages, such as simple technology and readily available low-cost raw materials, this system has strong potential for its application in rural areas for acquiring clean water.

https://doi.org/10.1021/acsomega.1c05925
ACS Omega 2021, 6, 35104−35111

■ ASSOCIATED CONTENT

Supporting Information

The Supporting Information is available free of charge at https://pubs.acs.org/doi/10.1021/acsomega.1c05925.

Single crochet stitch method to make the base of the HFLA (MP4)

Top and side view of HFLA, thickness of the HFLA layer, light absorption mechanism of 2D−3D structures, and side application of HFLA (PDF)

■ AUTHOR INFORMATION

Corresponding Author

Bi Xu − *National Engineering Research Center for Dyeing and Finishing of Textiles, College of Chemistry, Chemical Engineering and Biotechnology, Donghua University, Shanghai 201620, China;* orcid.org/0000-0003-0137-2706; Email: xubi@foxmail.com

Authors

Muhammad Javed − *National Engineering Research Center for Dyeing and Finishing of Textiles, College of Chemistry, Chemical Engineering and Biotechnology, Donghua University, Shanghai 201620, China;* orcid.org/0000-0003-3882-5908

Sippi Pirah − *National Engineering Research Center for Dyeing and Finishing of Textiles, College of Chemistry, Chemical Engineering and Biotechnology, Donghua University, Shanghai 201620, China*

Yonghe Xiao − *National Engineering Research Center for Dyeing and Finishing of Textiles, College of Chemistry, Chemical Engineering and Biotechnology, Donghua University, Shanghai 201620, China*

Yilan Sun − *National Engineering Research Center for Dyeing and Finishing of Textiles, College of Chemistry, Chemical Engineering and Biotechnology, Donghua University, Shanghai 201620, China*

Yating Ji − *National Engineering Research Center for Dyeing and Finishing of Textiles, College of Chemistry, Chemical Engineering and Biotechnology, Donghua University, Shanghai 201620, China*

Muhammad Zubair Nawaz − *College of Science and Shanghai Institute of Intelligent Electronics and Systems, Donghua University, Shanghai 201620, China;* orcid.org/0000-0002-0598-4315

Zaisheng Cai − *National Engineering Research Center for Dyeing and Finishing of Textiles, College of Chemistry, Chemical Engineering and Biotechnology, Donghua University, Shanghai 201620, China;* orcid.org/0000-0002-5648-9330

Complete contact information is available at: https://pubs.acs.org/10.1021/acsomega.1c05925

Author Contributions

M.J.: methodology, conceptualization, writing, review, investigation, data curation, experiments, formal analysis, software, editing, original manuscript preparation, captured photos, and supplementary video. S.P.: formal analysis and investigation. Y.X.: formal analysis. Y.S.: formal analysis. Y.J.: formal analysis and software. M.Z.N.: conceptualization, methodology, writing, review, investigation, data curation, formal analysis, software, experiments, editing, and original manuscript preparation. Z.C.: project administrator and review. B.X.: supervision, project administrator, funding acquisition, and conceptualization.

Notes

The authors declare no competing financial interest.

■ ACKNOWLEDGMENTS

The work was supported by The Fundamental Research Funds for Central University (no. 2232020G-03) and China Postdoctoral Science Foundation (2019M661325).

■ REFERENCES

(1) Millstein, D.; Wiser, R.; Bolinger, M.; Barbose, G. The climate and air-quality benefits of wind and solar power in the United States. *Nat. Energy* **2017**, *2*, 17134.

(2) Renuka, H.; Enaganti, P. K.; Venkataraman, B. H.; Ramaswamy, K.; Kundu, S.; Goel, S. Submerged solar energy harvesting using ferroelectric Ti-doped BFO-based heterojunction solar cells. *Int. J. Energy Res.* **2021**, *45*, 20400−20412.

(3) Nawaz, M. Z.; Xu, L.; Zhou, X.; Shah, K. H.; Wang, J.; Wu, B.; Wang, C. CdS nanobelt-based self-powered flexible photodetectors with high photosensitivity. *Mater. Adv.* **2021**, *2*, 6031−6038.

(4) Nawaz, M. Z.; Xu, L.; Zhou, X.; Shah, K. H.; Yaqub, M.; Wang, J.; Wu, B.; Wang, C. Flexible Photodetectors with High Responsivity and Broad Spectral Response Employing Ternary SnxCd1-xS Micro-nanostructures. *ACS Appl. Electron. Mater.* **2021**, *3*, 4151−4161.

(5) Loeb, S.; Hofmann, R.; Kim, J.-H. Beyond the Pipeline: Assessing the Efficiency Limits of Advanced Technologies for Solar Water Disinfection. *Environ. Sci. Technol. Lett.* **2016**, *3*, 73−80.

(6) Guo, Y.; Javed, M.; Li, X.; Zhai, S.; Cai, Z.; Xu, B. Solar-Driven All-in-One Interfacial Water Evaporator Based on Electrostatic Flocking. *Adv. Sustainable Syst.* **2021**, *5*, 2000202.

(7) Yu, F.; Guo, Z.; Xu, Y.; Chen, Z.; Irshad, M. S.; Qian, J.; Mei, T.; Wang, X. Biomass-Derived Bilayer Solar Evaporator with Enhanced Energy Utilization for High-Efficiency Water Generation. *ACS Appl. Mater. Interfaces* **2020**, *12*, 57155−57164.

(8) Song, G.; Yuan, Y.; Liu, J.; Liu, Q.; Zhang, W.; Fang, J.; Gu, J.; Ma, D.; Zhang, D. Biomimetic Superstructures Assembled from Au Nanostars and Nanospheres for Efficient Solar Evaporation. *Adv. Sustainable Syst.* **2019**, *3*, 1900003.

(9) Zhou, Y.; Duan, C.; Huang, Z.; Ma, Q.; Liao, G.; Liu, F.; Qi, X. Stable flexible photodetector based on FePS3/reduced graphene oxide heterostructure with significant enhancement in photoelectrochemical performance. *Nanotechnology* **2021**, *32*, 485203.

(10) Yu, F.; Ming, X.; Xu, Y.; Chen, Z.; Meng, D.; Cheng, H.; Shi, Z.; Shen, P.; Wang, X. Quasimetallic Molybdenum Carbide−Based Flexible Polyvinyl Alcohol Hydrogels for Enhancing Solar Water Evaporation. *Adv. Mater. Interfaces* **2019**, *6*, 1901168.

(11) Dao, V.-D.; Vu, N. H.; Thi Dang, H.-L.; Yun, S. Recent advances and challenges for water evaporation-induced electricity toward applications. *Nano Energy* **2021**, *85*, 105979.

(12) Kabeel, A. E.; El-Agouz, S. A. Review of researches and developments on solar stills. *Desalination* **2011**, *276*, 1−12.

(13) Dao, V.-D.; Choi, H.-S. Carbon-Based Sunlight Absorbers in Solar-Driven Steam Generation Devices. *Glob. Chall.* **2018**, *2*, 1700094.

(14) Dao, V.-D.; Vu, N. H.; Choi, H.-S. All day Limnobium laevigatum inspired nanogenerator self-driven via water evaporation. *J. Power Sources* **2020**, *448*, 227388.

(15) Dao, V.-D. An experimental exploration of generating electricity from nature-inspired hierarchical evaporator: The role of electrode materials. *Sci. Total Environ.* **2021**, *759*, 143490.

(16) Tao, P.; Ni, G.; Song, C.; Shang, W.; Wu, J.; Zhu, J.; Chen, G.; Deng, T. Solar-driven interfacial evaporation. *Nat. Energy* **2018**, *3*, 1031−1041.

(17) Konch, T. J.; Dutta, T.; Buragohain, M.; Raidongia, K. Remarkable Rate of Water Evaporation through Naked Veins of Natural Tree Leaves. *ACS Omega* **2021**, *6*, 20379−20387.

(18) Singh, S. C.; ElKabbash, M.; Li, Z.; Li, X.; Regmi, B.; Madsen, M.; Jalil, S. A.; Zhan, Z.; Zhang, J.; Guo, C. Solar-trackable super-wicking black metal panel for photothermal water sanitation. *Nat Sustain* **2020**, *3*, 938−946.
(19) Wu, S.; Gong, B.; Yang, H.; Tian, Y.; Xu, C.; Guo, X.; Xiong, G.; Luo, T.; Yan, J.; Cen, K.; Bo, Z.; Ostrikov, K. K.; Fisher, T. S. Plasma-Made Graphene Nanostructures with Molecularly Dispersed F and Na Sites for Solar Desalination of Oil-Contaminated Seawater with Complete In-Water and In-Air Oil Rejection. *ACS Appl. Mater. Interfaces* **2020**, *12*, 38512−38521.
(20) Zhang, X.; Peng, Y.; Shi, L.; Ran, R. Highly Efficient Solar Evaporator Based On a Hydrophobic Association Hydrogel. *ACS Sustain. Chem. Eng.* **2020**, *8*, 18114−18125.
(21) Yang, Y.; Sui, Y.; Cai, Z.; Xu, B. Low-Cost and High-Efficiency Solar-Driven Vapor Generation Using a 3D Dyed Cotton Towel. *Glob. Chal.l* **2019**, *3*, 1900004.
(22) Gan, W.; Wang, Y.; Xiao, S.; Gao, R.; Shang, Y.; Xie, Y.; Liu, J.; Li, J. Magnetically Driven 3D Cellulose Film for Improved Energy Efficiency in Solar Evaporation. *ACS Appl. Mater. Interfaces* **2021**, *13*, 7756−7765.
(23) Yuan, B.; Zhang, C.; Liang, Y.; Yang, L.; Yang, H.; Bai, L.; Wei, D.; Wang, W.; Wang, Q.; Chen, H. A Low-Cost 3D Spherical Evaporator with Unique Surface Topology and Inner Structure for Solar Water Evaporation-Assisted Dye Wastewater Treatment. *Adv. Sustainable Syst.* **2021**, *5*, 2000245.
(24) Dao, V.-D.; Vu, N. H.; Yun, S. Recent advances and challenges for solar-driven water evaporation system toward applications. *Nano Energy* **2020**, *68*, 104324.
(25) Maurya, A.; Singh, S. Promoting Export of Crochet Laces from India: Role of Export Promotion Council of Handicrafts. *FIIB Business Review* **2017**, *6*, 20−24.
(26) Guo, R.; Lin, J.; Narayanan, V.; McCann, J. Representing Crochet with Stitch Meshes. *Symp Comput Fab* **2020**, *4*, 1−8.
(27) Zhang, L.; Huang, Y.; Dong, H.; Xu, R.; Jiang, S. Flame-retardant shape memory polyurethane/MXene paper and the application for early fire alarm sensor. *Compos. B Eng.* **2021**, *223*, 109149.
(28) Huang, Y.; Jiang, S.; Liang, R.; Sun, P.; Hai, Y.; Zhang, L. Thermal-triggered insulating fireproof layers: A novel fire-extinguishing MXene composites coating. *Chem. Eng. J.* **2020**, *391*, 123621.
(29) Zhang, T.; Fang, L.; Lin, N.; Wang, J.; Wang, Y.; Wu, T.; Song, P. Highly transparent, healable, and durable anti-fogging coating by combining hydrophilic pectin and tannic acid with poly(ethylene terephthalate). *Green Chem.* **2019**, *21*, 5405−5413.
(30) Bachchan, A. A.; Nakshbandi, S. M. I.; Nandan, G.; Kumar Shukla, A.; Dwivedi, G.; Kumar Singh, A. Productivity enhancement of solar still with phase change materials and water-absorbing material. *Mater. Today: Proc.* **2021**, *38*, 438−443.
(31) Chang, Q.; Guo, Z.; Shen, Z.; Li, N.; Xue, C.; Zhang, H.; Hao, C.; Yang, J.; Hu, S. Interaction Promotes the Formation and Photothermal Conversion of Carbon Dots/Polydopamine Composite for Solar-Driven Water Evaporation. *Adv. Mater. Interfaces* **2021**, *8*, 2100332.
(32) Ghasemi, H.; Ni, G.; Marconnet, A. M.; Loomis, J.; Yerci, S.; Miljkovic, N.; Chen, G. Solar steam generation by heat localization. *Nat. Commun.* **2014**, *5*, 4449.
(33) Liu, K.; Zhang, W.; Cheng, H.; Luo, L.; Wang, B.; Mao, Z.; Sui, X.; Feng, X. A Nature-Inspired Monolithic Integrated Cellulose Aerogel-Based Evaporator for Efficient Solar Desalination. *ACS Appl. Mater. Interfaces* **2021**, *13*, 10612−10622.
(34) Gao, C.; Zhu, J.; Bai, Z.; Lin, Z.; Guo, J. Novel Ramie Fabric-Based Draping Evaporator for Tunable Water Supply and Highly Efficient Solar Desalination. *ACS Appl. Mater. Interfaces* **2021**, *13*, 7200−7207.
(35) Wang, Z.; Wu, X.; He, F.; Peng, S.; Li, Y. Confinement Capillarity of Thin Coating for Boosting Solar-Driven Water Evaporation. *Adv. Funct. Mater.* **2021**, *31*, 2011114.
(36) Ni, G.; Zandavi, S. H.; Javid, S. M.; Boriskina, S. V.; Cooper, T. A.; Chen, G. A salt-rejecting floating solar still for low-cost desalination. *Energy Environ. Sci.* **2018**, *11*, 1510−1519.

https://doi.org/10.1021/acsomega.1c05925
ACS Omega 2021, 6, 35104−35111